TOXICOLOGICAL SCIENCES **64,** 28–40 (2001)

The Role of Oxidative Stress in Indium Phosphide-Induced Lung Carcinogenesis in Rats

Barbara C. Gottschling,* Robert R. Maronpot,† James R. Hailey,† Shyamal Peddada,† Cindy R. Moomaw,† James E. Klaunig,* and Abraham Nyska†,[1]

**Indiana University School of Medicine, Division of Toxicology, Department of Pharmacology and Toxicology, 635 Barnhill Drive, MS 1021, Indianapolis, Indiana 46202; and †National Institute of Environmental Health Sciences, Laboratory of Experimental Pathology, 111 T. W. Alexander Drive, MD B3-06, Research Triangle Park, North Carolina 27709*

Received February 26, 2001; accepted June 14, 2001

Indium phosphide (IP), widely used in the microelectronics industry, was tested for potential carcinogenicity. Sixty male and 60 female Fischer 344 rats were exposed by aerosol for 6 h/day, 5 days/week, for 21 weeks (0.1 or 0.3 mg/m^3; stop exposure groups) or 105 weeks (0 or 0.03 mg/m^3 groups) with interim groups (10 animals/group/sex) evaluated at 3 months. After 3-month exposure, severe pulmonary inflammation with numerous infiltrating macrophages and alveolar proteinosis appeared. After 2 years, dose-dependent high incidences of alveolar/bronchiolar adenomas and carcinomas occurred in both sexes; four cases of squamous cell carcinomas appeared in males (0.3 mg/m^3), and a variety of nonneoplastic lung lesions, including simple and atypical hyperplasia, chronic active inflammation, and squamous cyst, occurred in both sexes. To investigate whether inflammation-related oxidative stress functioned in the pathogenesis of IP-related pulmonary lesions, we stained lungs of control and high-dose animals immunohistochemically for four markers indicative of oxidative stress: inducible nitric oxide synthase (i-NOS), cyclooxygenase-2 (COX-2), glutathione-*S*-transferase Pi (GST-Pi), and 8-hydroxydeoxyguanosine (8-OHdG). Paraffin-embedded samples from the 3-month and 2-year control and treated females were used. i-NOS and COX-2 were highly expressed in inflammatory foci after 3 months; at 2 years, all four markers were expressed in nonneoplastic and neoplastic lesions. Most i-NOS staining, mainly in macrophages, occurred in chronic inflammatory and atypical hyperplastic lesions. GST-Pi and 8-OHdG expression occurred in cells of carcinoma epithelium, atypical hyperplasia, and squamous cysts. These findings suggest that IP inhalation causes pulmonary inflammation associated with oxidative stress, resulting in progression to atypical hyperplasia and neoplasia.

Key Words: **indium phosphide; oxidative stress; inflammation; lung carcinogenesis; immunohistochemistry.**

Indium phosphide (IP), a dark gray powder or brittle metallic solid, belongs to the main group III of nonessential heavy metals and has been used in industry since the 1940s. Indium-containing compounds, e.g., indium arsenide and IP, are now used extensively in the microelectronics industry to manufacture semiconductors, injection lasers, solar cells, photodiodes, and light-emitting diodes and have been proposed as replacements for silicon in computer microchips (Blazka *et al*., 1994).

Because of its recent widespread usage, IP was selected for chronic toxicity investigations by the National Toxicology Program (NTP). Three-month exposure of rats by inhalation of IP at doses of 0, 1, 3, 10, 30, or 100 mg/m^3 resulted in a spectrum of inflammatory and proliferative lesions in the lungs of all exposed groups. These changes consisted of alveolar proteinosis, chronic inflammation, interstitial fibrosis, and alveolar epithelial hyperplasia (NTP, 2000).

Inhalation exposure to 0.03 mg/m^3 for 2 years, or 0.1 or 0.3 mg/m^3 for 21 weeks (exposure stopped at 21 weeks) was associated with increased incidences of alveolar and bronchiolar adenomas and bronchiolar carcinomas in rats of both sexes. Squamous cell carcinoma of the lung occurred in four male rats exposed to 0.3 mg/m^3 (NTP, 2000). A spectrum of inflammatory and proliferative lesions of the lung was observed in all exposed groups of both sexes. This paper deals with IP-related lung pathology; additional information can be found in the NTP technical report (NTP, 2000).

Exposure by inhalation to particles like asbestos (Muhle and Pott, 2000) or crystalline silica (Ding *et al*., 2000) is known to be associated with the development of lung tumors in rats (Nehls *et al*., 1997). Inflammation, in conjunction with the production of reactive oxygen species (ROS) and enhanced epithelial cell proliferation, has been proposed as the mechanism of this particle-induced tumor formation (Mossman, 2000). Interactions of xenobiotics with several enzyme systems have resulted in the formation of free-radical intermediates, which are further able to activate molecular oxygen to superoxides (Mason, 1982). Reactive oxygen is recognized as an important factor in gene expression by serving as a second messenger in signal transduction pathways. This function in cell signaling has been well established for H_2O_2 and O_2-, as well as $NO^{\bullet}$. At least 127 genes and signal-transducting proteins have been reported to be redox-sensitive (Allen and

[1] To whom correspondence should be addressed. Fax: (919) 541-7666. E-mail: nyska@niehs.nih.gov.

Tresini, 2000; Lander, 1997). Many of these cell-signaling pathways are known to be involved in cell proliferation, differentiation, and apoptosis. The imbalance of these biological end points is an important step in the development of cancer. The current concept of oxidative stress emphasizes the balance between oxidants and antioxidants; an imbalance of too few oxidants and too many antioxidants is considered oxidative stress. Chronic, prolonged inflammation is associated with the release of highly reactive oxygen and nitrogen species from inflammatory cells. These reactive molecules interact with DNA in proliferating epithelium to produce permanent genomic alteration (De Marzo *et al*., 1999). High $NO^{\bullet}$ levels in inflammation are cytotoxic to viruses and bacteria, but are also able to damage cellular organelles and cause further chronic inflammation (Nathan and Xie, 1994). Excessive amounts of $NO^{\bullet}$ have been found to be cytotoxic in several cell lines (Messmer *et al*., 1994), but also protective against apoptosis in others (Kim *et al*., 1997). Another function of $NO^{\bullet}$ is scavenging superoxide radicals produced by inflammation, thereby inhibiting lipid peroxidation (Rubbo *et al*., 2000).

The lung is more susceptible to oxidative injury than any other organ in the body because of constant exposure to air that might contain toxic particles or oxidant gases such as nitrogen oxide or ozone (Nehls *et al.*, 1997). Lungs have a high rate of blood perfusion, which makes them more likely to be exposed to xenobiotics (Vallyathan and Shi, 1997). Chemical-induced carcinogenesis by inhalation was recently reviewed by Emmendoerffer *et al*. (2000), who examined confounding factors including the extent of the inflammatory response on lung neoplastic development.

To address our proposal that IP causes lung tumors via oxidative stress from inflammatory cells, we stained lungs of control and high-dose animals immunohistochemically to localize four different markers considered to be indicative of oxidative stress: inducible nitric oxide (i-NOS), cyclooxygenase 2 (COX-2), glutathione *S*-transferase Pi (GST-Pi), and 8-hydroxydeoxyguanosine (8-OHdG). Tissues used in this investigation were paraffin-embedded lungs from the 2-year NTP study (NTP, 2000).

MATERIALS AND METHODS

Chemicals. Indium phosphide, obtained in three lots from Johnson Matthey, Inc. (Ward Hill, MA), displayed a purity greater than 99% identified by X-ray diffraction analyses.

Aerosol generation and exposure system. The study laboratory designed stainless steel inhalation exposure chambers (Hartford Systems Division of Lab Products, Inc., Aberdeen, MD), ensuring the maintenance of uniform aerosol concentrations throughout. The total active mixing volume of each chamber was 1.7 m^3. Uniformity of aerosol chamber concentration was evaluated every 2 to 4 months and found acceptable throughout the study. Additional technical details concerning IP exposure are given in the NTP report (NTP, 2000).

Animals. Sixty male and 60 female F344/N 4-week-old rats (Taconic Farms, Germantown, NY) per exposure group were quarantined for approximately 14 days. Their health was monitored during the studies according to the protocols of the NTP Sentinel Animal Program. Animals were housed individually; feed (except during exposure) and water were available *ad libitum*.

The rats were exposed to aerosols of IP at levels of 0, 0.03, 0.1, or 0.3 mg/m^3 for 6 h/day, 5 days/week, for 21 weeks (0.1 or 0.3 mg/m^3 groups) or 105 weeks (0 or 0.03 mg/m^3 groups), with interim groups (10/group/sex) evaluated at 3 months. Animals in the 0.1 and 0.3 mg/m^3 groups were maintained on filtered air from exposure termination at week 21 until the end of the studies. Exposure to IP was stopped in these dosed groups because of a 1.6- to 2.1-fold increase in lung weights and the severity of the lung lesions after 3-month exposure (NTP, 2000).

Pathology. Complete necropsies and microscopic examinations were performed on 0 and 0.3 mg/m^3 interim study rats at 3 months, and all remaining rats at the end of the study. Heart, right kidney, liver, lung (left and right lobe), right testis, and thymus were examined and weighed from 0.03 and 0.1 mg/m^3 interim study rats at 3 months. At necropsy, all organs and tissues were examined for grossly visible lesions, and all major tissues were fixed and preserved in 10% neutral buffered formalin, processed and trimmed, embedded in paraffin, sectioned to a thickness of 4–6 μm, and stained with hematoxylin and eosin (H&E) for microscopic examination. A quantitative assessment for lung pathology was performed to evaluate the severity of the different findings (Cherniack *et al*., 1991).

Immunohistochemical investigation. For the immunohistochemical evaluations, paraffin-embedded samples were taken from the lungs of female rats only, as the pulmonary damage appeared virtually the same in both sexes. To investigate the most severe lesions, only lungs of the high-dose animals were stained immunohistochemically. Samples from each of the following groups were used:

- Three-month interim sampling: lungs from seven rats from each of the control and high-dose (0.3 mg/m^3) groups.
- Two-year terminal sampling: lungs from 10 rats of the control group and 18 animals of the high-dose (0.3 mg/m^3) group. These 18 animals were selected to have a minimum of seven animals per specific lesion (inflammation, hyperplasia, adenoma, carcinoma, atypical hyperplasia, squamous cyst) to have a sufficient number of samples for statistical evaluation.

Immunohistochemistry was performed using the avidin-biotin-peroxidase method. Sections were stained with one of the following antibodies: i-NOS (Transduction Laboratories, Lexington, KY), COX-2 (Caymen Chemical, Ann Arbor, MI), GST-Pi (BioGenex, San Ramon, CA), or 8-OHdG (Japan Institute for the Control of Aging, Haruoka, Fukuroi City, Japan).

i-NOS and COX-2. Following dehydration through a series of graded alcohols, all slides were placed in 1X Automation Buffer (AB) (Biomeda, Foster City, CA) and blocked for endogenous peroxidase activity with 3% H_2O_2 for 15 min. Heat-induced epitope retrieval for all slides began by incubation in 1X citrate buffer, pH 6.0 (Biocare Medical, Walnut Creek, CA). Slides stained for i-NOS were placed in a steamer (Black & Decker, Brockville, Ontario, Canada) for 30 min, cooled for 10 min, rinsed in water, and placed in buffer. Slides stained for COX-2 were heated for 5 min in a microwave oven at 50% power for a total of two cycles. Between cycles, fresh citrate buffer (50 ml) was added. After microwaving, the slides were allowed to cool for 15 min, rinsed in distilled water, and placed in 1X AB buffer. All incubations were carried out in a humidified chamber at room temperature (RT°). Slides were blocked with 5% normal goat serum for 20 min (Jackson Immunoresearch, West Grove, PA), then incubated with the primary antibody, i-NOS 1:100 or COX-2 1:300, for 1 h. Normal rabbit serum (Jackson Immunoresearch, West Grove, PA) was used as the negative control. For i-NOS staining, the positive control was LPS-treated rat liver. For COX-2 staining, the positive control was mouse vas deferens (ductus deferens). Slides were adequately washed in 1X AB buffer; incubated with the secondary antibody, biotinylated goat anti-rabbit IgG (for i-NOS 1:400, for COX-2 1:500; Vector Laboratories, Burlingame, CA) for 30 min, washed again, then labeled with an avidin-biotin complex (Vector Elite Kit) for 30 min. Slides were washed in 1X AB buffer, counterstained with Harris hematoxylin (Harelco, Gibbstown, NJ),

TABLE 1
Incidences of Non-neoplastic Lesions of the Lungs in Female Rats at Three-Month Interim Evaluation in the Two-Year IP Inhalation Study

	0 mg/m^3	0.03 mg/m^3	0.1 mg/m^3	0.3 mg/m^3
Number of animals[a]	10	10	10	10
Chronic active inflammation[b]	2 (1.0)[c]	10* (1.0)	10* (1.6)	10* (3.4)
Foreign body	0	8* (1.0)	10* (1.6)	10* (2.7)
Alveolus, proteinosis	0	9* (1.0)	10* (2.7)	10* (4.0)
Alveolar epithelium, hyperplasia[d]	0	5* (1.0)	1* (1.0)	7* (1.6)

[a] Tissue examined microscopically.
[b] Number of animals with lesion.
[c] Average severity grade of lesions in affected animals: 1 = minimal, 2 = mild, 3 = moderate, 4 = marked.
[d] All animals showed simple hyperplasia.
* Indicates significantly different from chamber control, using Fisher exact test ($p \leq 0.01$).

rinsed in water, rehydrated through alcohol to xylene, and coverslipped with Permount (Surgipath, Richmond, IL).

8-OHdG and GST-Pi. Following dehydration through a series of graded alcohols, the slides for 8-OHdG determination were placed in Bouin's fixative for 3 h at RT°, washed in 80% ethanol four times, then left therein overnight. Tissues were blocked for endogenous peroxidase activity with 0.3% H_2O_2 in methanol for 30 min and rinsed in PBS buffer. For denaturation of DNA, the slides were placed in 0.05 N NaOH in 40% ethanol for 12 min, rinsed in PBS, and incubated with 250 μg/ml RNase for 1 h. The RNase was rinsed off with PBS, and an incubation in 5% skim milk in PBS for 90 min followed. An avidin/biotin block (Vector Laboratories, Burlingame, CA) was applied for 20 min. The primary 8-OHdG antibody (IgG1, 20 μg/ml, 1:50) was then applied to the slides overnight at 4°C.

The GST-Pi slides were placed in PBS after dehydration; endogenous peroxidase was blocked by 3% H_2O_2 for 15 min, and slides were incubated with 5% skim milk for 90 min at RT°. The primary polyclonal rabbit anti-GST-Pi antibody (BioGenex, San Ramon, CA) was applied at 1:200 for 3 h at 37°C. All slides (GST-Pi and 8-OHdG) were then washed adequately in PBS and incubated with BioGenex biotin-labeled antimouse antibody followed by BioGenex streptavidin-conjugated peroxidase, each at 1:20 for 20 min at RT°. The peroxidase binding was demonstrated by the reaction with 3-amino-9-ethylcarbazole. Rinsing in deionized water and counterstaining with Meyer's hematoxylin followed. Tissue was covered with BioGenex SuperMount overnight and coverslipped with Eukitt® (Calibrated Instruments, Hawthorne, NY).

As a control for the specifity of the reaction for 8-OHdG, some slides were incubated with formamidopyrimidine DNA glycosylase (Fpg) protein, a trifunctional DNA base excision repair enzyme that removes a wide range of oxidatively damaged bases via N-glycosylase activity and cleaves both the 3′- and 5′-phosphodiester bonds of the resulting apurinic/apyrimidinic site. By application of the enzyme for 1 h prior to that of the primary antibody, a large amount of 8-OHdG in the tissue should be repaired and so not react with the primary antibody.

As a positive control for GST-Pi staining, livers were used from rats that were treated with diethylnitrosamine (DEN) over a period of 2 weeks, kept without treatment for 7 months for the development of liver foci, then treated with lipopolysaccharide for 1 week.

Grading of labeling. The immunopositivity of the sections was graded by two pathologists using a scale ranging from 0 (–) to 4 (++++). Only a strong specific immunohistochemical reaction was considered and graded as follows, with approximate percentages indicating those numbers of relevant cells showing a strong positive reaction: (0) = No specific immunohistologic reaction visible; (1) = 1 to 10% of relevant cells showing a strong positive reaction; (2) = Up to approximately 25%; (3) = Up to approximately 50%; (4) = More than approximately 50%.

In case of disagreement of single grades, an average was taken. The immunohistochemical reactivity of each histological category (normal tissue, atypical hyperplasia, chronic active inflammation, alveolar epithelium hyperplasia, squamous cyst, alveolar/bronchiolar carcinoma, alveolar/bronchiolar adenoma) was assessed separately.

Statistical analysis. For evaluation of the statistical significance of the immunopositivity, we used a new test procedure recently introduced by Peddada *et al.* (manuscript submitted) to detect a broad range of trends. This procedure is based upon a general methodology developed by Hwang and Peddada (1994). We first converted the data in terms of ranks, then estimated the mean ranks under the hypothesized trend. Using these trend estimates we obtained our test statistic, which is the difference between the largest mean rank and the smallest mean rank. The null distribution of this statistic was obtained by the bootstrap trend test, conservative for correlated data (Peddada *et al.*, manuscript submitted). For COX-2, 8-OHdG, and GST-Pi labelings, the hypothesis was that the immunopositivity increases from hyperplasia to adenoma to carcinoma to atypical hyperplasia to squamous cyst. For the i-NOS stain, the hypothesis asserted that the distribution of immunopositivity increases from adenoma to carcinoma to atypical hyperplasia. For i-NOS evaluation, we did not include hyperplasia and squamous cyst due to sparsity of data.

RESULTS

As only lungs from female rats were investigated immunohistochemically, only the pathology results from females are presented in this paper.

Survival and Body Weights

The survival rates of chamber controls and treated animals were approximately equal (NTP, 2000). The average body weights of exposed rats compared to chamber controls were similar (NTP, 2000).

Pulmonary Pathology

The lung weights of all groups of exposed female rats were significantly (1.2- to 2.2-fold) greater than those of the chamber controls after 3 months (NTP, 2000). Most exposed animals showed dose-dependent increased incidences of chronic active inflammation (Table 1), which is characterized by nu-

merous histiocytes and mononuclear inflammatory cells and fewer pleomorphonuclear (PMNL) inflammatory cells within the alveoli and interstitia (Figs. 1A–D). Other changes included the presence of foreign bodies (indium phosphide particles) visible as black dots within the alveoli or macrophages (not shown), alveolar epithelial hyperplasia, and alveolar proteinosis (Table 1).

Inhalation exposure to 0.03 mg/m^3 (2 years), 0.1, or 0.3 mg/m^3 (exposure stopped at 21 weeks) was associated with increased incidences of alveolar and bronchiolar adenomas and carcinomas in rats of both sexes. Squamous cell carcinomas of the lung occurred in four males exposed to 0.3 mg/m^3. In all exposed groups of males and females, a spectrum of dose-dependent inflammatory and proliferative pulmonary lesions was observed, including chronic inflammation, alveolar epithelial hyperplasia and squamous metaplasia, atypical hyperplasia, squamous cyst, alveolar proteinosis, and interstitial fibrosis (Table 2).

Alveolar epithelial hyperplasia was indicated by increased numbers of epithelial cells lining the alveolar walls with normal alveolar architecture remaining intact.

Chronic inflammation (Figs. 1E–F) consisted of accumulations of alveolar macrophages with foamy cytoplasm, occasional multinucleated giant cells and cholesterol clefts, cell debris, and some neutrophils. A thickening of the alveolar interstitium and the overlying pleura was observed frequently in connective tissues. Alveolar proteinosis, characterized by diffuse homogeneous to granular deposition of eosinophilic material, was noted within the alveolar lumen, mostly around the areas of chronic inflammation. Scattered black dots (IP particles) less than 1 μm in diameter were found within alveoli and phagocytic cells.

Atypical proliferation of alveolar/bronchiolar epithelium with fibrous components (Figs. 1I and 1J and 2A–D) was also found in these animals. The lesions, whose size ranged from a few hundred micrometers to more than 1 cm in diameter, were round with a central fibrous core containing dispersed alveolar structures lined with uniformly cuboidal epithelial cells. Aggregates of chiefly necrotic inflammatory cells were present in adjacent alveoli and often within the glandular structures. At the periphery, the proliferative lesions contained one to many layers of epithelium, which sometimes extended into neighboring alveoli. These cells showed pleomorphism and sometimes contained mitotic figures. Small lesions were seen close to areas of chronic inflammation. Small lesions with some peripheral epithelial proliferation were diagnosed as "atypical hyperplasia," whereas larger lesions with more epithelial proliferation and cellular polymorphism and/or local invasion were diagnosed as alveolar/bronchiolar adenoma or carcinoma.

Squamous metaplasia of alveolar/bronchiolar epithelium, which was not evaluated independently by immunohistochemical staining but was considered part of the chronic inflammatory process, consisted of replacement of normal alveolar epithelium by flattened squamous epithelial cells that sometimes produced keratin. Cystic squamous lesions exhibited a somewhat thickened edge of epithelium around a large amount of keratin (Figs. 2E–H).

Alveolar/bronchiolar adenomas consisted of clearly outlined masses compressing and surrounding normal lung tissue and exhibited acinar, papillary, and/or compact structure. These epithelial cells within adenomas were mostly of one form and resembled hyperplastic epithelial cells.

Alveolar/bronchiolar carcinomas (Figs. 2I and 2J) displayed a more heterogeneous pattern, cellular pleomorphism, and atypia with local invasion or metastasis.

Immunohistological Evaluation

The immunohistochemical markers revealed distinct patterns of localization (Tables 3 and 4). Staining for i-NOS resulted in a cytoplasmic expression, mainly in macrophages, not in epithelial cells (Figs. 1A, 1B, 1E, 1F, 1I, and 1J). COX-2 immunolabeling demonstrated a cytoplasmic concentration of chromogen in macrophages and epithelial cells included within lesions (Figs. 1C and 1D and Figs. 2D, 2G, 2H, and 2J). GST-Pi was expressed mainly in the cytoplasm and partially in the nuclei of epithelial cells (Figs. 1G and 2A, 2B, 2E, and 2I); few macrophages expressed GST-Pi. 8-OHdG was localized within nuclei of epithelial cells (Figs. 1H and 2C and 2F); few macrophages expressed 8-OHdG.

In the control group, after 3 months the average expression of i-NOS was graded 2–3 in the cytoplasm of macrophages, which appeared with a frequency of approximately 1–2 macrophages/alveolus. The macrophages in the control animals were smaller than those in the highest-dose group. COX-2 was expressed between grades 2 and 4 in macrophage cytoplasm and minimally (grade 1 in three animals) in bronchial epithelium. Two control animals demonstrated immunopositivity of GST-Pi (grades 1–2) in macrophage cytoplasm, and two others in bronchial epithelium (grades 1–2). 8-OHdG (grade 1) was found in macrophages of one animal.

After 3 months, treated animals (Table 3) of the highest-dose group (0.3 mg/m^3) manifested relatively extensive i-NOS (average grade 4.0; Figs. 1A and 1B) and COX-2 staining (average grade 2.8; Figs. 1C and 1D) within infiltrating macrophages in sites of chronic active inflammation, the major lesion in these animals. Although portions of some lesions showed high grades of staining of GST-Pi, its overall expression was only present in a small percentage of cells in chronic active inflammation and epithelial hyperplasia. 8-OHdG, expressed only in some animals, appeared in a small percentage of cells within chronic active inflammation. Alveolar proteinosis, diagnosed in all treated animals of this group, showed a relatively high percentage of COX-2–positive area within the proteinaceous material (average grade 4.0).

In the control group after 2 years (Table 4), i-NOS was expressed in macrophages of two animals with chronic inflammation (grade 2.8) and also in a single carcinoma (grade 3.0).

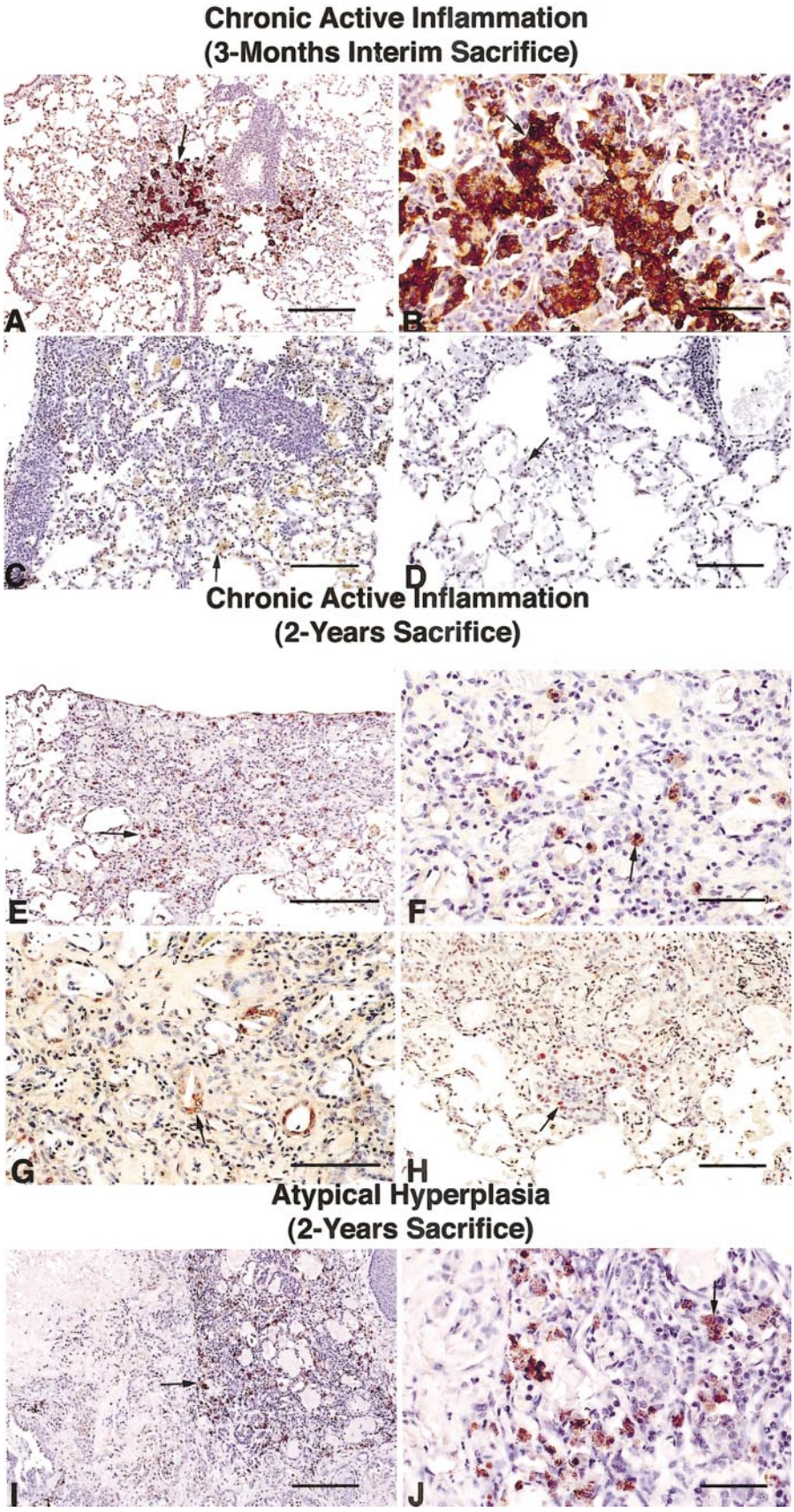
Chronic Active Inflammation
(3-Months Interim Sacrifice)
A
B
C
D
Chronic Active Inflammation
(2-Years Sacrifice)
E
F
G
H
Atypical Hyperplasia
(2-Years Sacrifice)
I
J

TABLE 2
Incidences of Neoplasms and Non-neoplastic Pulmonary Lesions in Female Rats in Two-Year IP Inhalation Study

	0 mg/m^3	0.03 mg/m^3	0.1 mg/m^3	0.3 mg/m^3
Number of animals[a]	50	50	50	50
Atypical hyperplasia[b]	0	8** (2.8)[c]	8** (2.9)	39** (3.8)
Chronic active inflammation	10 (1.0)	49** (3.0)	50** (2.6)	49** (3.9)
Alveolar epithelium, metaplasia	0	46** (3.3)	47** (2.4)	48** (3.8)
Foreign body	0	49** (2.1)	50** (1.8)	50** (2.0)
Alveolus, proteinosis	0	49** (3.7)	47** (2.0)	50** (3.8)
Interstitium, fibrosis	0	48** (2.9)	50** (2.6)	49** (3.9)
Alveolar epithelium, hyperplasia	8 (1.5)	15 (2.1)	22** (2.0)	16* (1.8)
Squamous metaplasia	0	2 (1.5)	1 (2.0)	4 (2.5)
Squamous cyst	0	1 (4.0)	1 (4.0)	10** (3.6)
Alveolar/bronchiolar adenoma, multiple	0	1	1	1
Adenoma (includes multiple)	0	7**	5*	19**
Carcinoma, multiple	0	1	0	7**
Carcinoma (includes multiple)	1	3	1	11**
Alveolar/bronchiolar adenoma or carcinoma[d]				
Overall rate[e]	1/50 (2%)	10/50 (20%)	6/50 (12%)	26/50 (52%)
Adjusted rate[f]	2.3%	23.5%	13.5%	58.8%
Terminal rate[g]	1/34 (2%)	6/31 (19%)	6/36 (17%)	23/34 (68%)
First incidence (days)	735 (T)[h]	694	735 (T)	519
Poly-3 test[i]	$p < 0.001$	$p = 0.004$[j]	$p = 0.063$	$p < 0.001$

[a] Number of animals examined microscopically.
[b] Number of animals with lesion.
[c] Average severity grade of lesions in affected animals: 1 = minimal, 2 = mild, 3 = moderate, 4 = marked.
[d] Historical incidence of alveolar/bronchiolar adenoma or carcinoma: 5/299.
[e] Number of animals with neoplasms per number with lungs examined microscopically.
[f] Poly-3 test accounts for differential mortality in animals that do not reach terminal sacrifice—estimated neoplasm incidence after adjustment for intercurrent mortality.
[g] Incidence at terminal kill.
[h] Not applicable; no neoplasm in group.
[i] Beneath the chamber control incidence are *p* values associated with trend test (0.03 mg/m^3 group excluded); beneath exposed group incidences are *p* values corresponding to pairwise comparisons between chamber controls and exposed group. Poly-3 test as above.
[j] Statistical value not computable.
* Indicates significantly different ($p \leq 0.05$) from chamber control group by Fisher exact test.
** Indicates significantly different ($p \leq 0.01$) from chamber control group by Fisher exact test.
(T) Terminal sacrifice.

COX-2 was localized in two animals in epithelium of alveolar epithelial hyperplasia (grade 2.5), in macrophages of one animal showing chronic inflammation (grade 1.0), and in epithelium of one carcinoma (grade 3.0). GST-Pi was localized in the epithelium of alveolar hyperplasia (grade 1.5) in two animals, chronic inflammation (grade 0.5) in four animals, and carci-

FIG. 1. (A–D) Representative photomicrographs demonstrating localization of i-NOS, GST-Pi, 8-OHdG, and COX-2 in different lesions induced in female rats exposed to 0.3 mg/m^3 IP in 3-month and 2-year inhalation exposure study. Staining was performed on formalin-fixed tissues using specific monoclonal antibodies (see Materials and Methods section.). Strong red or brownish nuclear or cytoplasmic staining indicates presence of antigen. + = immunohistochemical positivity; – = negativity. Chronic active inflammation produced by 3-month IP exposure; lesions characterized by accumulation of mixed inflammatory cells (lymphocytes, macrophages, and fewer neutrophils) within alveoli and interstitium, associated with regenerative alveolar epithelial hyperplasia. (A) i-NOS; macrophages (cytoplasm, arrow) +. Bar 200 μm. (B) i-NOS; macrophages (cytoplasm, arrow) +; bar 50 μm. (C, D) COX-2; in (C), macrophages (cytoplasm, arrow) +; (D) negative control (incubated with rat IgG rather than primary antibody) of same area (macrophage –, arrow). Both: bar 100 μm. (E–H) Chronic inflammation produced by 2-year IP exposure; lesions characterized by accumulation of alveolar macrophages with foamy cytoplasm, occasional multinucleated giant cells, cholesterol clefts, cell debris, and few neutrophils; alveolar interstitium variably thickened by dense fibrous connective tissue (fibrosis); alveolar proteinosis most prominent in these areas. (E) i-NOS; macrophages (cytoplasm, arrow) +. Bar 200 μm. (F) i-NOS; macrophages (cytoplasm, arrow) +. Bar 50 μm. (G) GST-Pi; epithelium (cytoplasm, arrow) +. Bar 100 μm. (H) 8-OHdG; epithelium (nuclei, arrow) +. Bar 100 μm. Atypical hyperplasia produced by 2-year IP exposure. Lesions vary in size, have rounded outline and central fibrous core containing dispersed (alveolar) structures lined by uniformly cuboidal epithelial cells, aggregates of mostly necrotic inflammatory cells seen within adjacent alveoli, and, often, glandular structures. Peripherally, fibroproliferative lesions have one to several epithelial layers, frequently forming papillary projections. (I) i-NOS; macrophages (cytoplasm, arrow) +. Bar 200 μm. (J) i-NOS; macrophages (cytoplasm, arrow) +. Bar 50 μm.

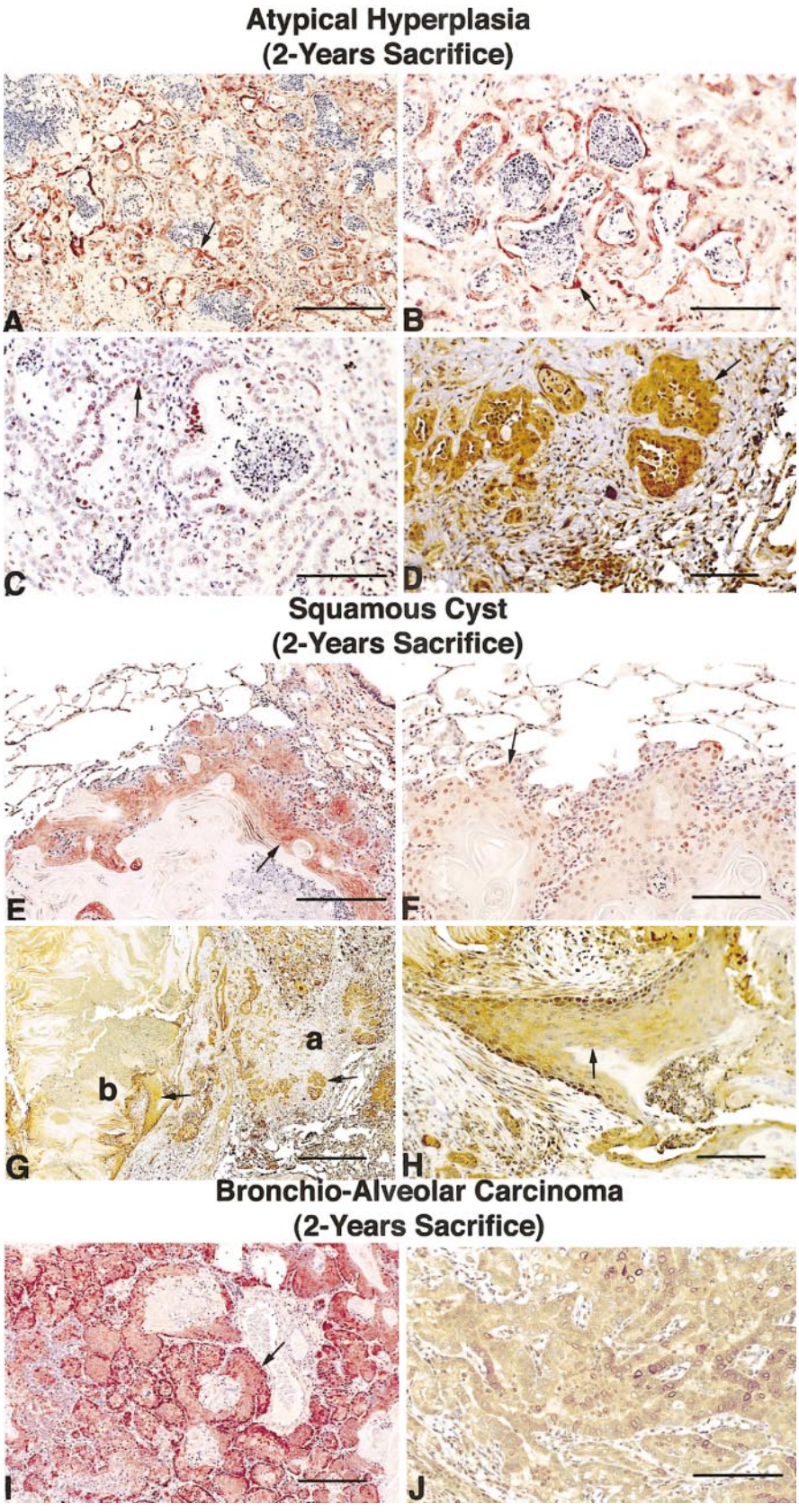
Atypical Hyperplasia
(2-Years Sacrifice)
A
B
C
D
Squamous Cyst
(2-Years Sacrifice)
E
F
a
b
G
H
Bronchio-Alveolar Carcinoma
(2-Years Sacrifice)
I
J

TABLE 3
Immunohistochemical Staining Results in Pulmonary Lesions in Epithelial Cells and Macrophages after Three-Month IP Exposure (0.3mg/m^3)

Lesion	i-NOS	COX-2	GST-Pi	8-OHdG
Epithelial cells				
Chronic inflammation	0.00 (7)	0.00 (7)	0.00 (7)	0.00 (7)
Alveolar epithelial hyperplasia	0.00 (7)	1.07 ± 1.24[a] (7)	0.14 ± 0.38 (7)	0.00 (7)
Macrophages				
Chronic inflammation	4.00 ± 0.00 (7)	2.79 ± 0.70 (7)	1.07 ± 0.19 (7)	0.64 ± 0.63 (7)
Alveolar epithelial hyperplasia	0.00 (7)	0.43 ± 1.13 (7)	0.29 ± 0.49 (7)	0.00 (7)
Proteinosis				
Alveolar proteinosis	0.00 (7)	3.86 ± 0.38 (7)	0.00 (7)	0.00 (7)

Note. Data in parentheses equals the number of animals identified with epithelial cells, macrophages, or proteinosis in the specific lesions; seven animals were evaluated for control group and seven for the exposed group. Grades ranged from 0–4 (see Materials and Methods section.). Control animals ($n = 7$) did not show any non-neoplastic or neoplastic pulmonary lesions.

[a]Means of immunohistochemical grading (0–4) ± standard deviation.

noma in one animal (grade 4.0) in which the macrophages expressed GST-Pi (grade 2.5). 8-OHdG was localized in epithelium of alveolar hyperplasia (grade 0.5) in two animals and chronic inflammation (grade 0.6) in four animals.

After 2-year exposure (Table 4), i-NOS was expressed mostly in lesions containing macrophages, including a few adenomas, most carcinomas, atypical hyperplasias (Figs. 1I and 1J), and, most prominently, chronic inflammatory lesions (Figs. 1E and 1F). COX-2 was expressed in most adenomas in epithelium and macrophages, all carcinomas in epithelium and macrophages (Fig. 2J), squamous cysts in epithelium (Figs. 2G and 2H), atypical hyperplasias in epithelium and macrophages (Fig. 2D), chronic active inflammation in epithelium and macrophages, alveolar epithelial hyperplasias in epithelium, and alveolar proteinosis. GST-Pi was observed chiefly in epithelial cells but seldom in macrophages. It was localized in the epithelium of all adenomas, squamous cysts (Fig. 2E), atypical hyperplasias (Figs. 2A and 2B), and chronic active inflammations (Fig. 1G), all but one carcinoma (Fig. 2I), and half of the alveolar epithelial hyperplasias. 8-OHdG, rarely expressed in macrophages, was seen mainly in the epithelium of a few carcinomas, most adenomas, atypical hyperplasias (Fig. 2C) and alveolar epithelial hyperplasias, all chronic active inflammations (Fig. 1H), and all squamous cysts but one (Fig. 2F).

Staining patterns were noted for each type of lesion. Adenomas expressed all four markers in average grades of about 2, whereas carcinomas expressed all except 8-OHdG to a slightly higher degree, indicating that the relative percentage of stained area in carcinomas was higher. Atypical hyperplasias (Figs. 1I and 1J and 2A–D) expressed i-NOS, COX-2, and GST-Pi with grades of about 3, and 8-OHdG staining was graded about 2. Squamous cysts (Figs. 2E–H) exhibited, respectively, grades 4, 3, 4, and 2 for i-NOS, COX-2, GST-Pi, and 8-OHdG. Chronic active inflammations (Figs. 1E–H) expressed i-NOS and COX-2 with an average grade of 3, and GST-Pi and 8-OHdG with an average grade of 2. Alveolar epithelial hyperplasias expressed COX-2 at grade 3, and GST-Pi and 8-OHdG at grade 1. Alveolar proteinosis demonstrated COX-2 expression, on average, at grade 4, but no labeling for the other markers.

Statistical Evaluation

The staining data for the 3-month interim study and the control group of the 2-year study did not indicate the ne-

FIG. 2. Representative photomicrographs demonstrating localization of i-NOS, GST-Pi, 8-OHdG, and COX-2 in different lesions induced in female rats exposed to 0.3 mg/m^3 IP in 2-year inhalation exposure study. Staining was performed on formalin-fixed tissues using specific monoclonal antibodies (see Materials and Methods section.). Strong red or brownish nuclear or cytoplasmic staining indicates presence of antigen. + = immunohistochemical positivity; – = negativity. Atypical hyperplasia produced by 2-year IP exposure. Lesions vary in size, have rounded outline and central fibrous core containing dispersed (alveolar) structures lined by uniformly cuboidal epithelial cells, aggregates of mostly necrotic inflammatory cells seen within adjacent alveoli, and, often, glandular structures. Peripherally, fibroproliferative lesions have one to several epithelial layers, frequently forming papillary projections. (A) GST-Pi; epithelium (cytoplasm, arrow) +. Bar 200 μm. (B) GST-Pi; epithelium (cytoplasm, arrow) +. Bar 100 μm. (C) 8-OHdG; epithelium (nuclei, arrow) +. Bar 100 μm. (D) COX-2; epithelium (cytoplasm, arrow) +. Bar 100 μm. Squamous cysts produced by 2-year IP exposure, characterized by variably thick band of viable squamous epithelium with large central core of keratin. (E) GST-Pi; well differentiated squamous epithelium (cytoplasm, arrow) +. Bar 200 μm. (F) 8-OHdG; epithelium (nuclei, arrow) +. Bar 100 μm. (G) COX-2; atypical hyperplasia (a) and squamous cyst (b); epithelium (cytoplasm, arrow) +. Bar 500 μm. (H) COX-2; squamous cyst; well-differentiated epithelium (cytoplasm, arrow) +. Bar 100 μm. Bronchioalveolar carcinomas produced by 2-year IP exposure; heterogeneous growth pattern, cellular pleomorphism, and/or atypia apparent. (I) GST-Pi; well-differentiated squamous epithelium (cytoplasm, arrow) +. Bar 200 μm. (J) COX-2; papillary epithelium (cytoplasm) +. Bar 100 μm.

TABLE 4

Immunohistochemical Staining Results in Epithelial Cells, Macrophages, and Proteinosis of Pulmonary Lesions after Two-Year IP (Control and 0.3 mg/m^3) Exposure

Lesion	i-NOS	COX-2	GST-Pi	8-OHdG
Control group				
Epithelial cells				
Chronic inflammation	0.00 (2)	0.00 (1)	0.00 (4)	0.00 (4)
Alveolar epithelial hyperplasia	0.00 (2)	2.50 ± 0.71[a] (2)	1.50 ± 2.12 (2)	0.50 ± 0.71 (2)
Macrophages				
Chronic inflammation	2.75 ± 1.77 (2)	1.00 (1)	0.50 ± 0.58 (4)	0.63 ± 0.75 (4)
Alveolar epithelial hyperplasia	0.00 (2)	0.00 (2)	0.00 (2)	0.00 (2)
Epithelial cells				
Carcinoma	0.00 (1)	3.00 (1)	4.00 (1)	0.00 (1)
Macrophages				
Carcinoma	3.00 (1)	0.00 (1)	2.50 (1)	0.00 (1)
Exposed group				
Epithelial cells				
Alveolar epithelial hyperplasia	0.00 (6)	2.79 ± 0.57 (7)	0.57 ± 0.53 (7)	1.14 ± 0.75 (7)
Chronic inflammation	0.00 (18)	2.97 ± 0.47 (18)	2.08 ± 0.55 (18)	2.19 ± 0.25 (18)
Squamous cyst	0.00 (6)	2.90 ± 0.22 (5)	4.00 ± 0.00 (6)	2.10 ± 1.34 (5)
Atypical hyperplasia	0.13 ± 0.52 (15)	3.13 ± 0.52 (15)	2.87 ± 0.69 (15)	1.90 ± 0.93 (15)
Macrophages				
Chronic inflammation	3.03 ± 0.53 (18)	2.97 ± 0.47 (18)	0.11 ± 0.47 (18)	0.00 (18)
Squamous cyst	4.00 (1)	(0)	(0)	(0)
Atypical hyperplasia	3.00 ± 0.50 (15)	2.93 ± 0.96 (15)	0.00 (15)	0.00 (15)
Proteinosis				
Alveolar proteinosis	0.00 (18)	3.97 ± 0.12 (18)	0.00 (18)	0.00 (18)
Epithelial cells				
Adenoma	0.00 (6)	2.42 ± 1.24 (6)	1.75 ± 0.82 (6)	1.25 ± 0.76 (8)
Carcinoma	0.50 ± 1.41 (8)	2.75 ± 0.71 (8)	2.38 ± 1.27 (8)	0.94 ± 1.32 (8)
Macrophages				
Adenoma	2.17 ± 1.72 (6)	2.00 ± 1.58 (6)	0.00 (5)	0.00 (8)
Carcinoma	2.29 ± 1.25 (7)	2.81 ± 0.53 (8)	0.00 (8)	0.00 (8)

Note. Data in parentheses equals the number of animals with epithelial cells, macrophages, or proteinosis in the specific lesions. 10 animals were evaluated for control group and 18 for exposed group. Grades ranged from 0–4 (see Materials and Methods section).

[a] Means of immunohistochemical grading (0–4) ± standard deviation.

cessity of any statistical testing because of the sparsity of data in these groups. Results of the analyses performed on the other groups are summarized in Figure 3A–D). The trends were highly significant for 8-OHdG (Fig. 3D) and GST-Pi (Fig. 3C), with p values less than 0.05 in both cases, revealing an increase in immunopositivity from hyperplasia to adenoma to carcinoma to atypical hyperplasia to squamous cyst. We did not find a statistically significant trend for the i-NOS or COX-2 immunopositivity. Due to the paucity of data, we were unable to test for any correlation between the distribution of immunopositivity of GST-Pi and i-NOS. We did test for the equality of the two distributions in adenoma, carcinoma, and atypical hyperplasia using standard nonparametric rank tests for paired data. We concluded that there was no statistically significant difference among immunopositivity distributions of i-NOS and GST-Pi in adenoma ($n = 5$, $p = 0.75$), carcinoma ($n = 7$, $p = 1.00$), and atypical hyperplasia ($n = 15$, $p = 0.56$).

DISCUSSION

In this study, we sought to demonstrate that oxidative stress functions in IP-induced pulmonary carcinogenesis by performing immunolabeling on paraffin-embedded samples from female Fischer 344 rats following 2 years of IP inhalation. As fresh and frozen tissues were lacking, this advantageous methodology determined localization within specific cell types.

IP inhalation resulted in severe pulmonary inflammation, consisting of abundant, varied inflammatory cell infiltrations associated with free radicals (Emmendoerffer *et al*., 2000), which, if not scavenged, can affect cellular organelles and cause the formation of ROS. This oxidative stress, an important factor in gene expression, serves as a second messenger in signal transduction pathways (Allen and Tresini, 2000; Lander, 1997) and can induce cellular proliferation (Klaunig *et al*., 1998) that may lead to the induction of alveolar and bronchioalveolar tumors (Emmendoerffer *et al*., 2000; Mossman, 2000).

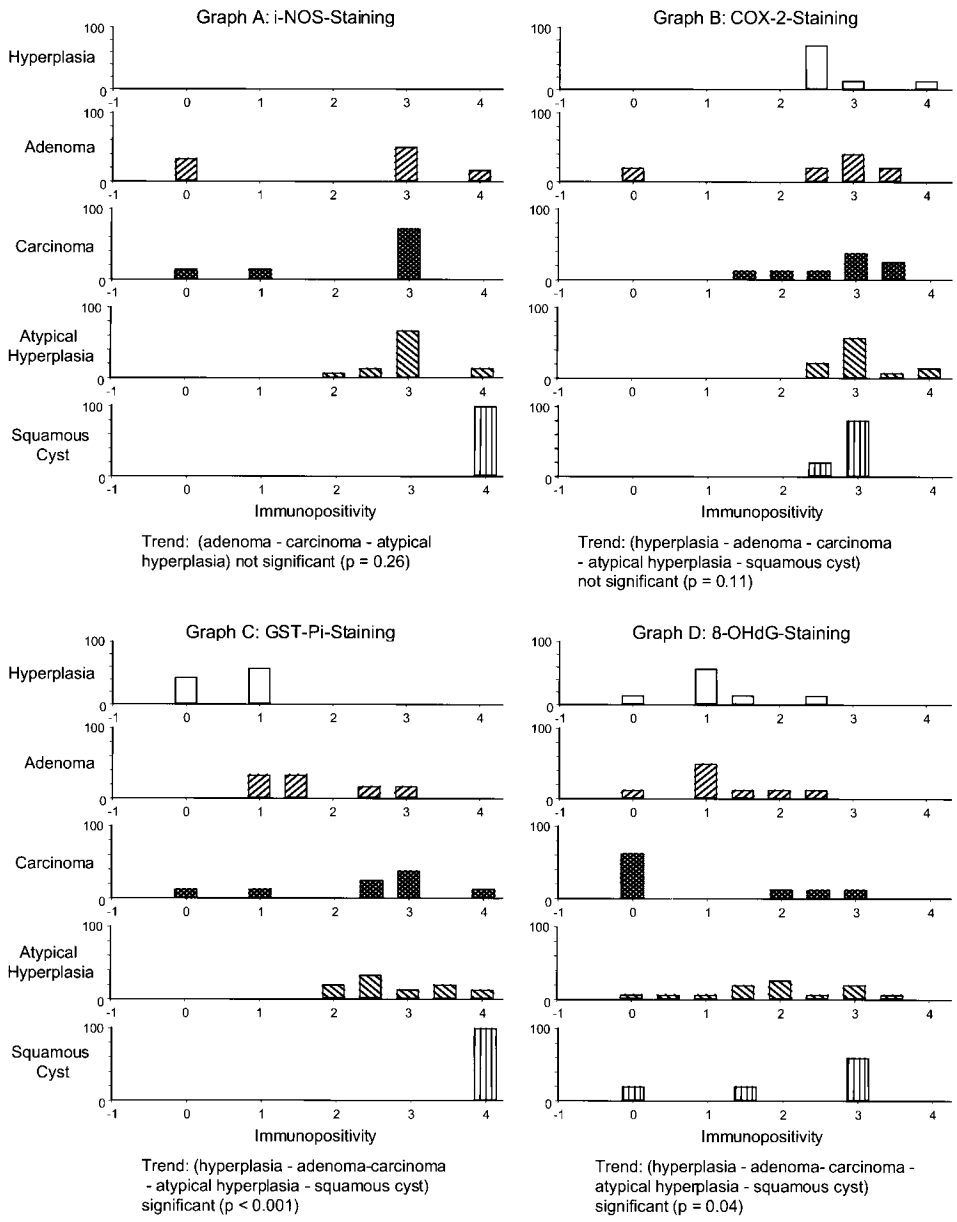

FIG. 3. Representative graphs A–D demonstrating relative frequency distribution of immunopositivity (grades 0–4, horizontal axes; see Materials and Methods section) of i-NOS, COX-2, GST-Pi, and 8-OHdG in hyperplasia, adenoma, carcinoma, atypical hyperplasia, and squamous cyst induced in female rats exposed to 0.3 mg/m^3 IP in 2-year inhalation exposure study. All graphs represent statistical analysis with nonparametric bootstrap trend test (see Materials and Methods section). (A) i-NOS; epithelial cells. (B) COX-2; macrophages. (C) GST-Pi; epithelial cells. (D) 8-OHdG; epithelial cells. Each column gives the relative number of animals (%) expressing specific grade of staining.

After 3 months of inhalation exposure, IP particles induced chronic inflammation, alveolar epithelial hyperplasia, and alveolar proteinosis. The severity of the lesions correlated with increasing concentrations of IP. Immunohistochemical staining of lungs exposed to 0.3 mg/m^3 showed i-NOS expression in inflammatory cells associated with minimal to mild alveolar hyperplasia. Accompanying inflammation, severe alveolar proteinosis developed, which showed a relatively large area of COX-2 positivity. In lung tumorigenesis, COX-2 expression has been found in mouse, rat, and humans (Bauer *et al*., 2000).

Pulmonary lesions changed in character with prolonged, 2-year exposure. Inflammatory lesions became extensive, severe, and associated with alveolar squamous metaplasia and development of atypical hyperplasias, squamous cysts, and alveolar and bronchiolar tumors. A similar development followed 2-year inhalation of cobalt sulfate (Bucher *et al*., 1999). The atypical fibroproliferative lesions consisted of a central fibrous core containing dispersed alveolar structures filled with inflammatory cells and exhibiting peripheral papillary epithelial proliferation. Typically, the squamous cysts were located at the periphery of atypical hyperplastic foci. Extensive chronic inflammation was either an integral part of these foci or occurred within a short distance. Atypical hyperplastic lesions seemed to progress to carcinomas. Depending on size, intrusion into neighboring alveoli, and presence of mitosis, these lesions were diagnosed as atypical hyperplasia or carcinoma. Rats administered IP intratracheally showed severe pulmonary inflammation and epithelial cell damage (Oda, 1997); similar

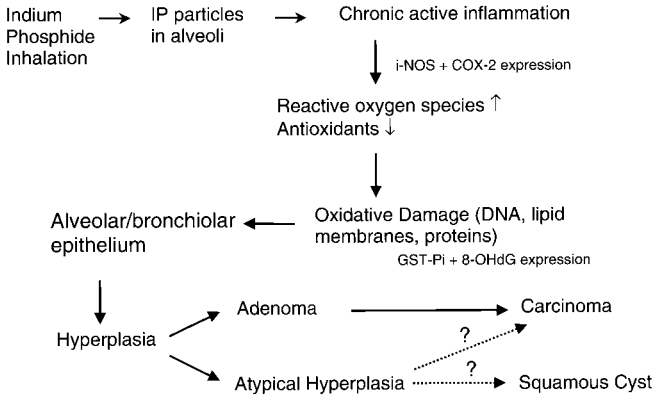

FIG. 4. Scheme of the proposed mechanism involved in lung carcinogenesis following IP inhalation in rats.

effects occurred with intratracheal instillation of IP or indium arsenide to Syrian hamsters (Tanaka *et al.*, 1996). Intratracheal administration of indium chloride to rats resulted in severe lung damage and fibrosis (Blazka *et al.*, 1994). We postulate an inflammation-carcinoma sequence in which chronic, prolonged inflammation is associated with the release of highly reactive oxygen and nitrogen species from inflammatory cells (Fig. 4).

Our data revealed strong induction of i-NOS and COX-2, leading to the production of $NO^{\bullet}$ radicals and prostaglandins that can have both beneficial and harmful effects on immune response and tissue injury (Fu *et al*., 1999). Three types of NOS-related enzymes are known. Inducible $NO^{\bullet}$ synthase (i-NOS), occurring abundantly in mononuclear phagocytes (Sharara *et al*., 1997), produces the highest amounts of $NO^{\bullet}$. $NO^{\bullet}$ overproduction is implicated in the pathogenesis of atherosclerosis, arthritis, asthma, cardiomyopathy, and cancer (Sandhu *et al*., 2000). The signaling functions of $NO^{\bullet}$ radicals involve reactions with heme prosthetic groups and reversible *S*-nitrosylations of protein thiols, or formation of peroxynitrite with its modifying actions on protein (Gabbita *et al*., 2000). i-NOS immunostaining revealed localization, mostly in macrophages, with highest average grades within chronic active inflammatory foci in the 3-month exposure group. Lesion progression suggests that the foreign bodies (IP) introduced into the lungs attracted macrophages for their digestion and removal and induced severe inflammation, which further enhanced $NO^{\bullet}$ production.

Cyclooxygenase catalyzes arachidonate metabolism and exists in two isoforms, COX-1 and COX-2, expressed in normal lung tissue of humans and experimental animals (Ermert *et al*., 1998). Prostanoids produced from arachidonic acid function in maintenance of airway smooth muscle tone, surfactant production, pulmonary hypertension, and vascular leakage. COX-1 is the "housekeeping" gene and COX-2 the inducible gene involved in inflammation and cellular proliferation (Herschman, 1994). COX-2 overexpression occurs in colorectal cancer, gastric cancer, breast cancer, and some lung cancers (Ochiai *et al*., 1999). Cyclooxygenase inhibitors, e.g., nonsteroidal antiinflammatory drugs (NSAIDS), reduce the size and number of colon adenomas (Reddy *et al*., 2000), and other COX-2-specific inhibitors prevent lung carcinogenesis (Rioux and Castonguay, 1998). In our investigation, the 3-month-exposure animals demonstrated a high percentage of COX-2–positive area within alveolar proteinosis (average grade 3.9). After 2-year exposure, COX-2 immunopositivity remained high (average grade 4.0) and showed elevation (approximately 3.0) in all lesions in epithelial cells and macrophages. These findings may confirm an association between COX-2 expression and lung carcinogenesis.

Two explanations could account for the failure of the trend test to show statistical significance for immunopositivity increase from hyperplasia to adenoma to carcinoma to atypical hyperplasia to squamous cyst in i-NOS and COX-2 localizations: bootstrap methodology, as implemented, may be conservative for correlated data, and small sample size can contribute to lower testing resolution.

Glutathione *S*-transferases (GSTs) contain multiple genes involved in detoxification and chemical activation (Eaton and Bammler, 1999). GSTs decrease the reactivity of electrophilic compounds with cellular macromolecules by catalyzing the nucleophilic attack of glutathione (Armstrong, 1997). GSTs detoxify endogenous products of lipid peroxidation and protect against oxidative stress in humans. Oxidative stress increases induced higher levels of GST-Pi whose overexpression can signify premalignant changes, like those found in rat preneoplastic hepatocytes forming GST-Pi-expressing foci. We observed that GST-Pi expression, mainly in epithelial cells, rarely macrophages, increased dramatically from 3 months to 2 years. After 3 months, the main pathological reaction was lung inflammation. Hyperplastic changes were minimal without epithelial atypia. After 2 years, GST-Pi expression occurred in all proliferative and neoplastic lesions, with average grades trending from hyperplasia to adenoma to carcinoma to atypical hyperplasia to squamous cyst. This correlation and the i-NOS and 8-OHdG staining indicated that the last three lesions are affected by oxidative stress. GST-Pi immunopositivity also indicated oxidative stress associated with premalignant or malignant characteristics of epithelial cells within lesions. GST-Pi expression in neoplasms has occurred in human lung carcinomas (Eimoto *et al*., 1988).

8-hydroxydeoxyguanosine (8-OHdG), a major indicator of DNA damage (Kasai and Nishimura, 1984) and oxidation, causes G-C → T-A transversions in bacteria and mammalian cells. Treatment of mice with diesel exhaust particles resulted in a dose-dependent increase in 8-OHdG in lung DNA (Ichinose *et al*., 1997). Immunohistochemical detection of 8-OHdG was first reported in paraffin-embedded rat livers (Takahashi *et al*., 1998). This immunohistochemical technique evaluating 8-OHdG does not discriminate between nuclear and mitochondrial DNA damage. A positive expression of 8-OHdG could represent mitochondrial DNA changes that do not lead to somatic mutations (Hensley *et al*., 2000). The progression in

immunopositivity of 8-OHdG was comparable to that of GST-Pi. After 3 months, no expression of this marker occurred in epithelial cells of alveolar hyperplasia. After 2-year exposure, 8-OHdG expression trended increasingly from hyperplasia to adenoma to carcinoma to atypical hyperplasia to squamous cysts—as we observed for GST-Pi staining, which showed, however, a slightly higher grading. The similar levels of expression of GST-Pi and 8-OHdG in proliferative and neoplastic lesions revealed that these indicators could be associated with oxidative stress. 8-OHdG, recently established as an immunohistochemical label in paraffin-embedded tissue (Takahashi *et al*., 1998), and used first in lung tissue in our laboratory, has become a useful marker.

Statistical analysis of the immunohistochemical grading indicated a trend of significantly higher relative frequency distribution of immunopositivity of GST-Pi and 8-OHdG in the atypical hyperplastic and squamous cystic lesions. This tendency suggests a significant oxidative stress–induced response in the epithelial cell due to abundant inflammatory cell infiltration and an ensuing overwhelming release of ROS. The lower grade of GST-Pi and 8-OHdG expression in carcinoma cells suggests that they are less protected from oxidative or electrophilic DNA damage and may be targets for genetic alterations and, hence, precursors for clonal expansion.

Our data support strongly our hypothesis that IP inhalation, effecting uptake of foreign particles into the lung, causes oxidative stress progressing to induction of pulmonary cancer (Fig. 4). Severe alveolar inflammation, marked by massive infiltration of macrophages and severe alveolar proteinosis, occurs subsequently. The inflammatory cells prompt an induction of i-NOS and COX-2, which secondarily produce $NO^{\bullet}$ and prostanoids. $NO^{\bullet}$ has proinflammatory qualities; COX-2 increases inflammation and cellular proliferation and inhibits apoptosis.

When exposure was terminated at 21 weeks and the results were examined after 2 years, female rats, while still showing chronic active inflammation and the presence of foreign bodies, had also developed proliferative and neoplastic pulmonary lesions. At this time point, the expression of all four biomarkers in different cell types indicated that an inflammatory response (i-NOS, COX-2), as well as oxidative stress (GST-Pi, 8-OHdG), still existed.

All of these observations lend strong credence to the supposition that oxidative stress plays a major role in the development of lung cancer from indium phosphide inhalation. Additional investigations using fresh lung tissue and measuring 8-OHdG by liquid chromatography, for example, might provide further confirmation of our findings.

ACKNOWLEDGMENTS

The authors are grateful to Dr. Po Chan and Ms. JoAnne Johnson from the National Institute of Environmental Health Sciences (NIEHS), and Dr. Michael Jokinen from Pathology Associates, Inc. for their helpful comments. We thank Ms. Natasha Clayton and Mr. Norris Flagler from the NIEHS for technical support, and Ms. Inta Kögel, from BASF-Corp. for important technical suggestions.

REFERENCES

Allen, R. G., and Tresini, M. (2000). Oxidative stress and gene regulation. *Free Radical Biol. Med.* **28,** 463–499.

Armstrong, R. N. (1997). Structure, catalytic mechanism, and evolution of the glutathione transferases. *Chem. Res. Toxicol.* **10,** 2–18.

Bauer, A. K., Dwyer-Nield, L. D., and Malkinson, A. M. (2000). High cyclooxygenase 1 (COX-1) and cyclooxygenase 2 (COX-2) contents in mouse lung tumors. *Carcinogenesis* **21,** 543–550.

Blazka, M. E., Dixon, D., Haskins, E., and Rosenthal, G. J. (1994). Pulmonary toxicity to intratracheally administered indium trichloride in Fischer 344 rats. *Fundam. Appl. Toxicol.* **22,** 231–239.

Bucher, J. R., Hailey, J. R., Roycroft, J. R., Haseman, J. K., Sills, R. C., Grumbein, S. L., Mellick, P. W., and Chou, B. J. (1999). Inhalation toxicity and carcinogenicity studies of cobalt sulfate. *Toxicol. Sci.* **49,** 56–67.

Cherniack, R. M., Colby, T. V., Flint, A., Thurlbeck, W. M., Waldron, J., Ackerson, L., and King, T. E., Jr. (1991). Quantitative assessment of lung pathology in idiopathic pulmonary fibrosis. The BAL Cooperative Group Steering Committee. *Am. Rev. Respir. Dis.* **144,** 892–900.

De Marzo, A. M., Marchi, V. L., Epstein, J. I., and Nelson, W. G. (1999). Proliferative inflammatory atrophy of the prostate: Implications for prostatic carcinogenesis. *Am. J. Pathol.* **155,** 1985–1992.

Ding, M., Shi, X., Castranova, V., and Vallyathan, V. (2000). Predisposing factors in occupational lung cancer: inorganic minerals and chromium. *J. Environ. Pathol. Toxicol. Oncol.* **19,** 129–138.

Eaton, D. L., and Bammler, T. K. (1999). Concise review of the glutathione *S*-transferases and their significance to toxicology. *Toxicol. Sci.* **49,** 156–164.

Eimoto, H., Tsutsumi, M., Nakajima, A., Yamamoto, K., Takashima, Y., Maruyama, H., and Konishi, Y. (1988). Expression of the glutathione *S*-transferase placental form in human lung carcinomas. *Carcinogenesis* **9,** 2325–2327.

Emmendoerffer, A., Hecht, M., Boeker, T., Mueller, M., and Heinrich, U. (2000). Role of inflammation in chemical-induced lung cancer. *Toxicol. Lett.* **112–113,** 185–191.

Ermert, L., Ermert, M., Goppelt-Struebe, M., Walmrath, D., Grimminger, F., Steudel, W., Ghofrani, H. A., Homberger, C., Duncker, H., and Seeger, W. (1998). Cyclooxygenase isoenzyme localization and mRNA expression in rat lungs. *Am. J. Respir. Cell. Mol. Biol.* **18,** 479–488.

Fu, S., Ramanujam, K. S., Wong, A., Fantry, G. T., Drachenberg, C. B., James, S. P., Meltzer, S. J., and Wilson, K. T. (1999). Increased expression and cellular localization of inducible nitric oxide synthase and cyclooxygenase 2 in *Helicobacter pylori* gastritis. *Gastroenterology* **116,** 1319–1329.

Gabbita, S. P., Robinson, K. A., Stewart, C. A., Floyd, R. A., and Hensley, K. (2000). Redox regulatory mechanisms of cellular signal transduction. *Arch. Biochem. Biophys.* **376,** 1–13.

Hensley, K., Robinson, K. A., Gabbita, S. P., Salsman, S., and Floyd, R. A. (2000). Reactive oxygen species, cell signaling, and cell injury. *Free Radic. Biol. Med.* **15,** 1458–1462.

Herschman, H. R. (1994). Regulation of prostaglandin synthase-1 and prostaglandin synthase-2. *Cancer Metastasis Rev.* **13,** 241–256.

Hwang, J., and Peddada, S. (1994). Confidence interval estimation subject to order restrictions. *Ann. Stat.* **22,** 67–93.

Ichinose, T., Yajima, Y., Nagashima, M., Takenoshita, S., Nagamachi, Y., and Sagai, M. (1997). Lung carcinogenesis and formation of 8-hydroxy-

deoxyguanosine in mice by diesel exhaust particles. *Carcinogenesis* **18,** 185–192.

Kasai, H., and Nishimura, S. (1984). Hydroxylation of deoxyguanosine at the C-8 position by ascorbic acid and other reducing agents. *Nucleic Acids Res.* **12,** 2137–2145.

Kim, Y. M., de Vera, M. E., Watkins, S. C., and Billiar, T. R. (1997). Nitric oxide protects cultured rat hepatocytes from tumor necrosis factor-alpha-induced apoptosis by inducing heat shock protein 70 expression. *J. Biol. Chem.* **272,** 1402–1411.

Klaunig, J. E., Xu, Y., Isenberg, J. S., Bachowski, S., Kolaja, K. L., Jiang, J., Stevenson, D. E., and Walborg, E. F., Jr. (1998). The role of oxidative stress in chemical carcinogenesis. *Environ. Health Perspect.* **106**(Suppl. 1), 289–295.

Lander, H. M. (1997). An essential role for free radicals and derived species in signal transduction. *FASEB J.* **11,** 118–124.

Mason, R. (1982). Free radical intermediates in the metabolism of toxic chemicals. In *Free Radicals in Biology,* Vol. 5 (W. Pryor, Ed.), pp.161–222. Academic Press, New York.

Messmer, U. K., Ankarcrona, M., Nicotera, P., and Brune, B. (1994). p53 expression in nitric oxide-induced apoptosis. *FEBS Lett.* **355,** 23–26.

Mossman, B. T. (2000). Mechanism of action of poorly soluble particulates in overload-related lung pathology. *Inhal. Toxicol.* **12,** 141–148.

Muhle, H., and Pott, F. (2000). Asbestos as reference material for fibre-induced cancer. *Int. Arch. Occup. Environ. Health* **73**(Suppl.), S53–S59.

Nathan, C., and Xie, Q. W. (1994). Nitric oxide synthases: Roles, tolls, and controls. *Cell* **78,** 915–918.

Nehls, P., Seiler, F., Rehn, B., Greferath, R., and Bruch, J. (1997). Formation and persistence of 8-oxoguanine in rat lung cells as an important determinant for tumor formation following particle exposure. *Environ. Health Perspect.* **105**(Suppl. 5), 1291–1296.

NTP (2000). Toxicology and carcinogenesis studies of indium phosphide (CAS No. 22398-80-7) in F344 rats and B6C3 F1 mice (inhalation studies). Department of Health and Human Services, Public Health Services, Bethesda.

Oda, K. (1997). Toxicity of a low level of indium phosphide (InP) in rats after intratracheal instillation. *Ind. Health* **35,** 61–68.

Ochiai, M., Oguri, T., Isobe, T., Ishioka, S., and Yamakido, M. (1999). Cyclooxygenase-2 (COX-2) mRNA expression levels in normal lung tissues and non-small cell lung cancers. *Jpn. J. Cancer Res.* **90,** 1338–1343.

Reddy, B. S., Hirose, Y., Lubet, R., Steele, V., Kelloff, G., Paulson, S., Seibert, K., and Rao, C. V. (2000). Chemoprevention of colon cancer by specific cyclooxygenase-2 inhibitor, celecoxib, administered during different stages of carcinogenesis. *Cancer Res.* **60,** 293–297.

Rioux, N., and Castonguay, A. (1998). Prevention of NNK-induced lung tumorigenesis in A/J mice by acetylsalicylic acid and NS-398. *Cancer Res.* **58,** 5354–5360.

Rubbo, H., Radi, R., Anselmi, D., Kirk, M., Barnes, S., Butler, J., Eiserich, J. P., and Freeman, B. A. (2000). Nitric oxide reaction with lipid peroxyl radicals spares alpha-tocopherol during lipid peroxidation. Greater oxidant protection from the pair nitric oxide/alpha-tocopherol than alpha-tocopherol/ascorbate. *J. Biol. Chem.* **275,** 10812–10818.

Sandhu, J. K., Privora, H. F., Wenckebach, G., and Birnboim, H. C. (2000). Neutrophils, nitric oxide synthase, and mutations in the mutatect murine tumor model. *Am. J. Pathol.* **156,** 509–518.

Sharara, A. I., Perkins, D. J., Misukonis, M. A., Chan, S. U., Dominitz, J. A., and Weinberg, J. B. (1997). Interferon (IFN)-alpha activation of human blood mononuclear cells *in vitro* and *in vivo* for nitric oxide synthase (NOS) type 2 mRNA and protein expression: Possible relationship of induced NOS2 to the anti- hepatitis C effects of IFN-alpha *in vivo*. *J. Exp. Med.* **186**, 1495–1502.

Takahashi, S., Hirose, M., Tamano, S., Ozaki, M., Orita, S., Ito, T., Takeuchi, M., Ochi, H., Fukada, S., Kasai, H., and Shirai, T. (1998). Immunohistochemical detection of 8-hydroxy-2′-deoxyguanosine in paraffin-embedded sections of rat liver after carbon tetrachloride treatment. *Toxicol. Pathol.* **26,** 247–252.

Tanaka, A., Hisanaga, A., Hirata, M., Omura, M., Makita, Y., Inoue, N., Ishinishi, N. (1996) Chronic toxicity of indium arsenide and indium phosphide to the lungs of hamsters. *Fukuoka Igaku Zasshi* **87,** 108–115.

Vallyathan, V., and Shi, X. (1997). The role of oxygen free radicals in occupational and environmental lung diseases. *Environ. Health Perspect.* **105**(Suppl. 1), 165–177.